AQUATIC CONSERVATION: MARINE AND FRESHWATER ECOSYSTEMS
Aquatic Conserv: Mar. Freshw. Ecosyst. **17**: 245–264 (2007)
Published online in Wiley InterScience
(www.interscience.wiley.com) DOI: 10.1002/aqc.833

The potential of L-band SAR for quantifying mangrove characteristics and change: case studies from the tropics

RICHARD M. LUCAS[a,*], ANTHEA L. MITCHELL[b], AKE ROSENQVIST[c], CHRISTOPHE PROISY[d], ALEX MELIUS[d,e] and CATHERINE TICEHURST[f]

[a] *Institute of Geography and Earth Sciences, The University of Wales, Aberystwyth, Ceredigion, United Kingdom*
[b] *School of Biological, Earth and Environmental Sciences, The University of New South Wales, Kensington, Sydney, Australia*
[c] *Japan Aerospace Exploration Agency (JAXA), Chuo-ku, Tokyo, Japan*
[d] *Institut de Recherches pour le Développement, UMR AMAP, Cayenne, French Guiana, France*
[e] *Centre d'études des Environnements Terrestres et Planétaires, Vélizy, France*
[f] *CSIRO Land and Water, Black Mountain Laboratories, Canberra, ACT, Australia*

ABSTRACT

1. The Japan Aerospace Exploration Agency's (JAXA) Advanced Land Observing Satellite (ALOS) L-band Phased Array Synthetic Aperture Radar (PALSAR), launched successfully in January 2006, will provide new data sets for coastal ecosystems mapping and change monitoring at local to global scales.
2. To evaluate L-band capability for mangrove applications, data acquired by the NASA airborne SAR (AIRSAR) and Japanese Earth Resources Satellite (JERS-1 SAR) over sites in Australia, French Guiana and Malaysia were used to demonstrate benefits for mapping extent and zones, retrieving biomass and structural attributes (e.g. height), and detecting change.
3. The research indicates that mapping is most effective where mangroves border non-forested areas and where differences in structure, as a function of species, growth stage and biomass distributions, occur between zones.
4. Using L-band SAR, biomass can be retrieved up to $\sim$100–140 Mg ha^{-1}, although retrieval is complicated by a noticeable decrease in L-band backscattering coefficient within higher ($\sim >$ 200 Mg ha^{-1}) biomass stands, particularly those with extensive prop root systems.
5. Change detection through multi-temporal comparison of data proved useful for mapping deforestation/regeneration and mangrove dynamics associated with changing patterns of sedimentation.
6. The research highlights the likely benefits and limitations of using ALOS PALSAR data and supports JAXA's Kyoto & Carbon (K&C) Initiative in promoting the use of these data for regional mangrove assessment.

KEY WORDS: mangroves; tropics; radar remote sensing; change detection

*Correspondence to: Richard M. Lucas, Institute of Geography and Earth Sciences, The University of Wales, Aberystwyth, Ceredigion, SY23 3DB, UK. E-mail: rml@aber.ac.uk

INTRODUCTION

Over the past few decades, mangroves worldwide have been subject to human disturbance, ranging from pollution to direct clearance (Alongi, 2002). As a result, their extent has been reduced from an estimated 19.8 million ha in the 1980s (Spalding *et al.*, 1997) to only 15 million ha by the end of 2000 (Food and Agricultural Organization, 2003). Many regions have also experienced an expansion or retraction of mangroves as a result of more subtle anthropogenic changes such as fluctuations in sea level and climate regimes associated with global warming and increased sedimentation along coastlines. The implications of such losses include a lowering of fish and invertebrate stocks (O'Grady *et al.*, 1996) and biodiversity in general (Blasco *et al.*, 1994) and greater exposure of coastlines to wave surges (Danielsen *et al.*, 2005).

Given the rapid changes that are occurring in many countries, mapping and monitoring of mangroves are paramount, and remote sensing data, particularly from space-borne sensors, represents a major source of information. A significant addition to the earth observation systems available for mangrove assessment is the Japan Aerospace Exploration Agency's (JAXA) Advanced Land Observing Satellite (ALOS) Phased Array L-band Synthetic Aperture Radar (PALSAR), which was launched successfully in January 2006. For a period anticipated to exceed 3 years, this sensor will be routinely providing near-global L-band ($\sim$23.5 cm wavelength) data at 10–20 m spatial resolution and repeat-pass interferometric observations (Rosenqvist *et al.*, 2004a). Global-scale mosaics of PALSAR data (50-m spatial resolution) will also be generated, which can be compared with 100-m spatial resolution mosaics generated previously for the mid-1990s using Japanese Earth Resources Satellite (JERS-1) L-band HH Synthetic Aperture Radar (Rosenqvist *et al.* 2000), thereby providing opportunities for intra/interannual and decadal assessments of change.

For these data to be used effectively for mapping and monitoring mangroves by national and international organizations, an understanding of the information content of SAR data acquired over mangroves at L-band is desirable. This paper therefore seeks to provide such understanding by conveying the results of case studies undertaken at mangrove sites across the tropics using a combination of airborne/space-borne SAR, wave scattering models and supportive fine spatial resolution remote sensing data and field measurements. Accordingly, it provides an informed insight into the capabilities of the ALOS PALSAR and also the preceding JERS-1 SAR, considers the importance of integrating observations from other sensors (e.g. Landsat), and presents options for mangrove assessment in the tropics at a regional to global scale.

SAR REMOTE SENSING OF MANGROVES: AN OVERVIEW

Most SAR operate at X, C, L or P-band frequencies (Table 1) and both polarimetric and interferometric systems are available. Polarized microwave signals can be horizontally (H) or vertically (V) transmitted and received, and co- and cross-polarized data are often referred to as HH or VV and HV (or VH) respectively. Polarimetric systems can measure, for each pixel and at the same time, the full scattering matrix from which the intensity (and backscattering coefficient (σ^{o}; expressed as decibels, dB) and phase of scattered fields can be derived for any polarization. Values of the backscattering coefficient relate to power quantities whereas

Table 1. Typical frequency bands used by SAR systems

Frequency bands	X-band	C-band	L-band	P-band
Frequency (GHz)	9.6	5.3	1.25	0.44
Wavelength (cm)	3.1	5.6	23.5	68.2

DOI: 10.1002/aqc

phase information is used to compute phase difference and correlation coefficient (coherence) between two signals. Polarimetry refers to the measurement of the phase difference and correlation between different polarizations, and measurement of phase allows the entire complex electromagnetic field to be recomposed. By contrast, interferometry refers to the measurement of the phase difference and correlation of two identical radar signals made from a slightly differing location and allows the generation of highly accurate Digital Elevation Models (DEMs; Madsen *et al*., 1993; Li *et al*., 2003) of the terrain or vegetated surfaces. Both techniques have demonstrated their usefulness in retrieving the structure and biomass of forested areas (e.g. Cloude and Pottier, 1997; Schmullius and Evans, 1997; Treuhaft and Cloude, 1999; Saatchi *et al*., 2001; Proisy *et al*., 2002; Pulliainen *et al*., 2003, Gaveau *et al*., 2003; Lucas *et al*., 2006).

For forests, including mangroves, the backscattering coefficient depends upon the interaction of microwaves of varying configuration (frequency, polarization and incidence angle) with components of the vegetation (e.g. leaves, branches and trunks) of varying size, dimension, density, orientation and dielectric constant (moisture content). Components of a size beneath that of the wavelength decrease (attenuate) the signal whilst those beyond or of the same order as the wavelength act as scatterers and increase the returned signal. At lower frequencies, the capacity of microwaves to penetrate the forest canopy, and hence interact with vegetative components increases. Compared with short-wavelength X-band or C-band, for example, the longer L-band microwaves have a greater likelihood of penetrating the foliage and small branches of the upper canopies of forests and interacting with woody trunk and larger branch components as well as the underlying surface (Tsolmon *et al*., 2002; Lucas *et al*., 2004). In addition, where microwaves penetrate through the forest volume, the underlying surface contributes to the backscattering coefficient as a function of moisture content and roughness.

The interaction of microwaves with different surfaces is often described with reference to the scattering mechanisms. Direct scattering, in its pure form, is when only one reflection occurs, which is typically specular (i.e. mirror-like). Diffuse scattering is where multiple reflections at differing angles occur and is, at the extreme, random. Depending upon the surfaces being imaged and the sensor configuration, scattering ranges from the direct to the diffuse. With this knowledge, several characteristics of mangroves need to be considered for better understanding and interpreting radar signatures. During low tides and dry seasons, the large amount of dead wood material and the complex root systems lead to a high surface roughness and an increase in diffuse scattering and overall backscattering. An exception is where an increase in scattering between taller vegetation and the ground surface occurs, as the roughness of the surface can decrease the backscattering coefficient by an exponential factor. The magnitude of the backscattering coefficient also varies with the nature of the exposed root systems as some species support large aerial woody roots (e.g. *Rhizophora* species) whilst others have pneumatophores (e.g. *Avicennia* species). Mangroves are, however, inundated regularly and as the underlying surface (whether soil or water) is smooth, specular scattering often dominates. In such cases, specularly reflected incident microwaves travelling at right angles (orthogonal) between tree trunks, for example, and the ground can interact and produce a strong double-bounce effect (MacDonald, 1980; Krohn *et al*., 1983; Ormsby *et al*., 1985; Imhoff, 1995a; Simard *et al*., 2002), which often increases the backscattering coefficient beyond the normal level of saturation (Mougin *et al*., 1999; Proisy *et al*., 2002). However, specular reflection depends on the architecture of the trees as well as the roughness of the underlying surface and is not observed in all mangroves. From many mangroves, the backscattering coefficient can be similar, as trees of the same species or growth stage often occur in relatively homogeneous zones that parallel the coastal margin. Similarities in backscattering coefficient are also frequently observed as the biomass of mangroves is often above the normal levels at which saturation of the backscattering coefficient occurs (typically 20–30 $\mathrm{Mg\,ha^{-1}}$, 60–100 $\mathrm{Mg\,ha^{-1}}$ and 100–150 $\mathrm{Mg\,ha^{-1}}$ for C-band, L-band and P-band respectively; Imhoff, 1995b) and can exceed 450 $\mathrm{Mg\,ha^{-1}}$.

Understanding the interaction of microwaves with different components of the forest is complex but can be assisted using models (Karam *et al*., 1995; Sun and Ranson, 1995) that simulate microwave scattering from the forest volume and/or underlying surface. These models are typically parameterized using ground-based

DOI: 10.1002/aqc

measurements (Fung *et al*., 1992; Ranson *et al*., 1997; Castel *et al*., 2001; Lucas *et al*., 2004) and decompose the backscattering coefficient into contributory scattering mechanisms (e.g. surface, surface-vegetation and vegetation interactions) which can be interpreted separately. Depending on the respective contribution of the surface, interactions and vegetation, statistical inversion of the empirical relationships can be justified or otherwise (Proisy *et al*., 2000).

SAR DATA FOR MANGROVE ASSESSMENT

Past use of L-band SAR data

Since the 1990s, publicly available L-band SAR systems have included the JERS-1 SAR (1992–1998), data from which were combined to produce regional mosaics as part of the Global Rain Forest Mapping (GRFM) and Global Boreal Forest Mapping (GBFM) projects (Rosenqvist *et al*., 2000, 2004a), and the Space Shuttle Imaging Radar (SIR-C) SAR (two missions in 1994; Hess *et al*., 1990; Pope *et al*., 1997). Key airborne sensors with polarimetric L-band capability have included the NASA JPL airborne SAR (AIRSAR; Milne, 2000; Milne and Tapley, 2002). Several of these studies suggested good promise for mangrove characterization, mapping and monitoring but, despite the availability of these L-band SAR data, only a handful of studies (e.g. Mougin *et al*., 1999; Pasqualini *et al*., 1999; Proisy *et al*., 2000; Mitchell, 2004; Rosenqvist *et al*., 2007) have directly investigated their use for this purpose. Part of this can be attributed to a lack of funding and hence the ability to undertake mangrove assessment, particularly in developing countries, as well as the practical difficulty in undertaking quantitative *in situ* measurements in mangrove swamps to support the interpretation of SAR data. The current generation of L-band sensors has also been operational for less than two decades and the available archives of data have, in many cases, been insufficiently separated in time for effective change detection. The lack of long-term data continuity and repeat coverage and restriction of some data sets for research purposes only (e.g. the AIRSAR and SIR-C) has also resulted in few operational developments.

The Advanced Land Observing Satellite (ALOS): observation strategies

Central to the promotion of ALOS is the Kyoto & Carbon (K&C) Initiative (Rosenqvist *et al*., 2003), which stems from the JERS-1 SAR GRFM and GBFM projects and defines an urgent need to supply eco-regional data of relevance to the international scientific community in support of carbon cycle science, global conventions (e.g. the Ramsar Convention) and conservation of the environment. A component of the K&C Initiative is to support regional mapping and monitoring of forested ecosystems, including mangroves, and identify key 'hot spots' where significant change (natural or anthropogenic) has already occurred or is expected to occur.

For this purpose, the ALOS platform provides an L-band polarimetric SAR (PALSAR), as well as two optical sensors (the AVNIR-2 and PRISM; Rosenqvist *et al*., 2004a), and offers more observation modes than its precursor, the JERS-1 satellite. The ALOS is positioned in a sun-synchronous orbit at 691 km, with a descending local Equator pass time at about 10:30 (22:30 in ascending mode) and orbital revisit period of 46 days. The PALSAR instrument is designed to operate with variable look angles, polarizations and resolutions, but to reduce user conflicts and promote regional scale homogeneity, the number of operational modes for PALSAR is limited to four, including HH single and HH + HV dual polarization (each with an incidence angle of 34.3° off nadir), full polarization, and wide swath ScanSAR mode (Table 2). The ALOS PALSAR data are expected to have an absolute and relative accuracy better than 1.5 dB and 1.0 dB respectively, which is anticipated to provide improved discrimination of land-cover types compared with the JERS-1 SAR.

DOI: 10.1002/aqc

Table 2. PALSAR default observation modes (Rosenqvist *et al.*, 2004a)

Polarization	Off-nadir angle (swath, resolution)	Coverage	Timing	Repetition
HH	34.3° (70 km, 10 m)	Global	Dec–Feb	Annual
HH + HV	34.3° (70 km, 20 m)	Global	Jun–Aug	Annual
HH + HV + VH + VV	21.5° (30 km, ~30 m)	Selected sites	Mar–May	2 years
ScanSAR-HH	(350 km, ~70 m)	Wetland sites	Jan–Dec	1–8 times per year

To establish a globally consistent archive of PALSAR data, in which all land areas are observed on an annual basis or better during the mission lifetime, a systematic data observation strategy has been implemented by JAXA (Rosenqvist *et al.*, 2004b). In the context of mangrove monitoring, global-scale PALSAR observations at fine spatial resolution over mangrove areas throughout the tropics and subtropics are planned at least twice per year during the ALOS mission life. These will be combined to generate regional mosaics at 50-m spatial resolution which can be compared with those generated previously at 100 m using JERS-1 SAR data. Such an observation strategy was carefully planned and implemented by researchers, including those associated with this paper, as part of the K&C Initiative.

SAR OBSERVATIONS OF MANGROVES: CASE STUDIES

To understand better the potential of the ALOS PALSAR and JERS-1 SAR data for characterizing, mapping and monitoring mangroves, the following sections present research outcomes from independent studies undertaken in northern Australia (two sites), French Guiana and Malaysia (Figure 1). The four case study regions (Table 3) have experienced a 'typical' range of natural and human pressures, including short- and long-term climate change, large area sediment redistribution, and human disturbance and clearance. These mangroves also contain a range of structures and biomass associated with different tree species, growth stages and forms.

Case study regions

The macro-tidal estuaries of the Alligator Rivers of Kakadu National Park (NP) in Australia's Northern Territory support significant expanses (~75 km) of mangroves (Brennan, 1996; Storrs and Finlayson, 1997). Mangrove species diversity is relatively low compared with counterparts in Southeast Asia, and distinct zones form in response to tidal inundation, freshwater flow, soil type and salinity (Blasco *et al.*, 1996). Along the West Alligator River, orthomosaics showing mangrove extent and Digital Elevation Models (DEMs) of canopy height were generated from 1991 stereo aerial photography (Lucas *et al.*, 2002; Mitchell *et al.*, in press). Species distributions (zones) were observed within hyperspectral Compact Airborne Spectrographic Imager (CASI-2) data acquired in July 2002. The mouth of the Daintree River in far north Queensland contains approximately 50 km^2 of estuarine vegetation, including mangroves, which have species similar to those observed in Kakadu NP. This mangrove system backs onto agricultural land (particularly sugar cane) and tropical rainforest, much of which is on steep terrain to the north. Along the 350-km coastline of French Guiana, the spatial and temporal distribution of mangroves is influenced primarily by sediment dispersal from the Amazon River (Fromard *et al.*, 1998). These mangroves, which are typical of those in the neotropical Atlantic region, are dominated by three mangrove species. The study focused on Crique Fouillée (4° 55′ N, 52° 21′ W), Sinnamary (5° 26′ N, 53° 02′ W), and Marais de Kaw (4° 45′ N, 52° 5′ W). SPOT and IKONOS sensor data were available (Fromard *et al.*, 2004). The mangroves in Perak state on the west coast of Peninsular Malaysia, as within many parts of Southeast Asia, are

DOI: 10.1002/aqc

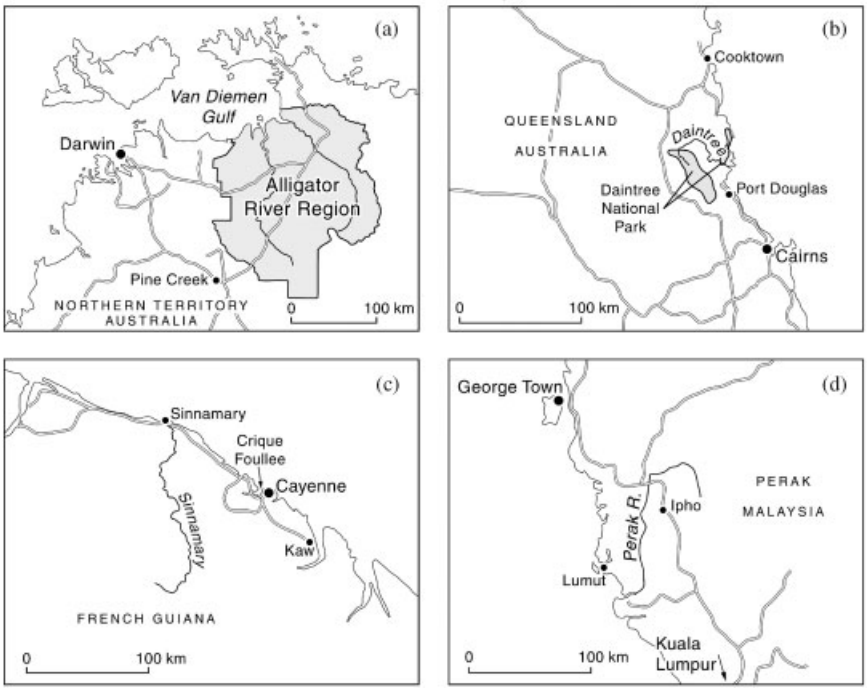

Figure 1. The location of coastal areas with mangroves in (a) Kakadu NP and (b) Daintree River NP in northern Australia, (c) French Guiana and (d) Perak, Malaysia.

Table 3. Characteristics of the mangrove regions and available SAR, optical and field data

Study site	Kakadu NP	Daintree River NP	Crique Fouillee	Perak
Country	Australia	Australia	French Guiana	Malaysia
Coordinates	S 12° E 130°	S 16° 18′ E 145° 5′	N 5° 15′ W 52° 45′	N 5° 5′ E 100° 30′
Airborne SAR	AIRSAR (1996, 2000)	AIRSAR (1996, 2000)	AIRSAR (1993)	
Space-borne SAR	JERS-1 SAR	JERS-1 SAR	JERS-1 SAR, SIR-C SAR	JERS-1 SAR
Other remote sensing data	Aerial photographs CASI	CASI	SPOT IKONOS	
Field data	1999, 2002	Prior to 1996	From 1993	1994
Tidal amplitude	5–6 m	5–6 m	3 m	n/a
Dominant species	*Rhizophora stylosa* *Avicennia marina* *Sonneratia alba*	*Rhizophora stylosa* *Cerips* *Brugeiria*	*Laguncularia racemosa* *Avicennia germinans* *Rhizophora* sp.	*Rhizophora* sp. *Avicennia*, sp. *Sonneratia* sp. *Brugueira* sp.
Other species	*Aegialitus corniculatus* *Bruguiera sp.* *Ceriops sp.*	*Xylocarpus sp* *Osbornia sp.*		
Disturbance	Storms, sea-level rise	Indirect human impacts, sea-level rise	Sedimentation and mudbank migration	Human-induced (aquaculture and logging)
Timescale of change	Interannual/decadal	Annual/decadal	Annual	Annual

DOI: 10.1002/aqc

experiencing extensive clearing largely to facilitate expansion of agricultural and aquaculture but also charcoal production. The area was included as it represents an example of rapid changes in mangrove extent associated with direct human activities.

A common link between all of the regions was that SAR data had been acquired for each between 1993 and 2000. Fully polarimetric AIRSAR data were acquired over all French Guiana sites in 1993 during the PACRIM Mission to South and Central America and over Kakadu NP in both 1996 and 2000 during the PACRIM I and II Missions to the Australasian region. During this latter mission, AIRSAR data were also collected over the Daintree NP in 1996 in so called 'TOPSAR' mode, with C-band interferometry (including correlation images) and L- and P-band polarimetry. In 2000, C- and L-band interferometry with P-band polarimetry as well as C-, L- and P-band polarimetry (in the opposite flight direction) were acquired. For the sites considered, the AIRSAR data were acquired at incidence angles ranging from 20° to 70° although the areas associated with the forest plots were imaged at incidence angles between 35° and 70°. For all regions, JERS-1 SAR data were acquired for one or several dates as part of the GRFM project.

Observations using L-band SAR over mangroves

Mangrove distributions and landscape setting

In most coastal regions, maps of mangrove distributions are a common requirement for management and conservation activities but the ability to discriminate using remote sensing data sets is dependent largely upon their similarity in appearance to adjoining land cover. Typical settings for mangroves were represented in the case study regions. The mangroves of the West Alligator River were bordered by water/wet mudflats on the seaward side, and dry, vegetation-free flats or samphires on the landward margin. The low values of σ^{o} from these two surfaces relative to that of mangroves permitted good discrimination using both JERS-1 SAR and AIRSAR L-band (all polarizations) data. However, the landward margins of the mangroves along the Daintree River were bordered by tropical forest or woodlands dominated by *Eucalyptus* or *Melaleuca* (paperbark) species, and the margins proved more difficult to identify within the available L-band SAR data because of similarities in the backscattering coefficient. Differences between mangroves and other forests were also not obvious within TOPSAR L-band interferometric correlation data, although the tall *Rhyzophora stylosa* mangroves displayed a noticeably lower correlation compared with other vegetation cover. Better discrimination was achieved, however, using TOPSAR C-band interferometric correlation data and was evident regardless of the height and density of the mangroves (Figure 2). Such differences were attributed to the relative homogeneity of both the cover and stand height of mangroves (and hence greater surface scattering) relative to the multi-layered canopy of the non-mangrove stands where height differences between trees were greater. The lesser discrimination using L-band interferometric correlation was attributed, in part, to the relatively short (2 m) baseline (distance between antennas) provided during the single over-flight. The use of a larger baseline (several hundred metres) provided through successive ALOS PALSAR over-flights might facilitate better discrimination, although diurnal and seasonal differences in, for example, forest moisture content between observations is likely to influence the interferometric signal by introducing temporal noise (Askne *et al.*, 1997).

In French Guiana, mangroves also bordered onto tropical rainforests as well as swamp, but in this case discrimination was achieved by applying thresholds to the L-band data which, at the mean incidence angle of 59°, were 3 dB lower for mangrove than rainforest although they varied by more than 10 dB (Proisy *et al.*, 1998). Poorer separation was achieved using C-band and X-band, particularly at co-polarizations. Swamp areas, which were often inundated, were discriminated as these exhibited decreasing backscattering coefficients at lower frequencies because of greater microwave penetration through the canopy of macrophytes and other herbaceous vegetation, and were easily separated using data thresholds. In Perak, the L-band HH backscattering coefficients associated with mature mangroves were approximately −10 to −11 dB and were typically 4 to 5 dB lower than adjacent rubber (*Hevea brasiliensis*) and oil palm (*Elaeis*

DOI: 10.1002/aqc

Figure 2. C-band interferometric correlation image of (a) the mangroves (white; higher correlation) and (b) *Melaleuca* (paperbark), *Acacia* and rainforests (grey) occurring in the Daintree River NP. The white box highlights an area where a mangrove/tropical forest boundary occurs.

guineensis) plantations, thereby accommodating their discrimination. These observations suggest that threshold techniques applied to L-band data, preferably within a time series, might be useful for separating mangrove from other vegetation (including forest) types at some sites, although these thresholds are unlikely to be consistent for routine application.

Zonation patterns

In terms of species composition and structure, mangroves are homogeneous relative to other forest systems and often exhibit a distinct zonation pattern in response to differing levels of tidal inundation, salinity and temperature (Mougin *et al.*, 1999). Using optical remote sensing data, and depending on the spatial resolution of the observing sensor, mangrove zones can often be distinguished because of differences in spectral reflectance between species. By contrast, discrimination using SAR requires that there is a difference in the structure (e.g. size, geometry) and dielectric constant of tree components between species. Establishing whether observed differences in the backscattering coefficient result from structural variation between species or growth stage and form (as a result of a varying response of the same species to environmental conditions) is an important consideration in their characterization.

Based on the CASI reflectance data for the West Alligator River and height statistics determined using a DEM generated from stereo aerial photography (Lucas *et al.*, 2002; Mitchell *et al.*, in press), the mangroves in the West Alligator River could be divided into five distinct zones (refer to Figure 3(a)). These zones consisted sequentially of landward forests dominated by *Avicennia marina* (up to 5 m; Zone I), a narrow strip of *Rhizophora stylosa* regrowth ($\sim$5–10 m; Zone II); a central spine dominated by *R. stylosa* (10–23 m; Zone III) and a mixed *R. stylosa* and *Sonneratia alba* community (10–15 m; Zone IV) which became increasingly dominated by *S. alba* towards the seaward margin as height declined to less than 10 m. An expansion of this seaward *S. alba* forest was evident in the 2002 CASI image but not the 1991 stereo photography (Zone V). Mangroves of lower height were associated with younger growth stages (e.g. in the case of *S. alba* on the seaward margin in Zone V and *R. stylosa* in Zone II) but also forests growing under less favourable growth conditions (i.e. the landward *A. marina* community; Zone I). In 1996 and 2000,

DOI: 10.1002/aqc

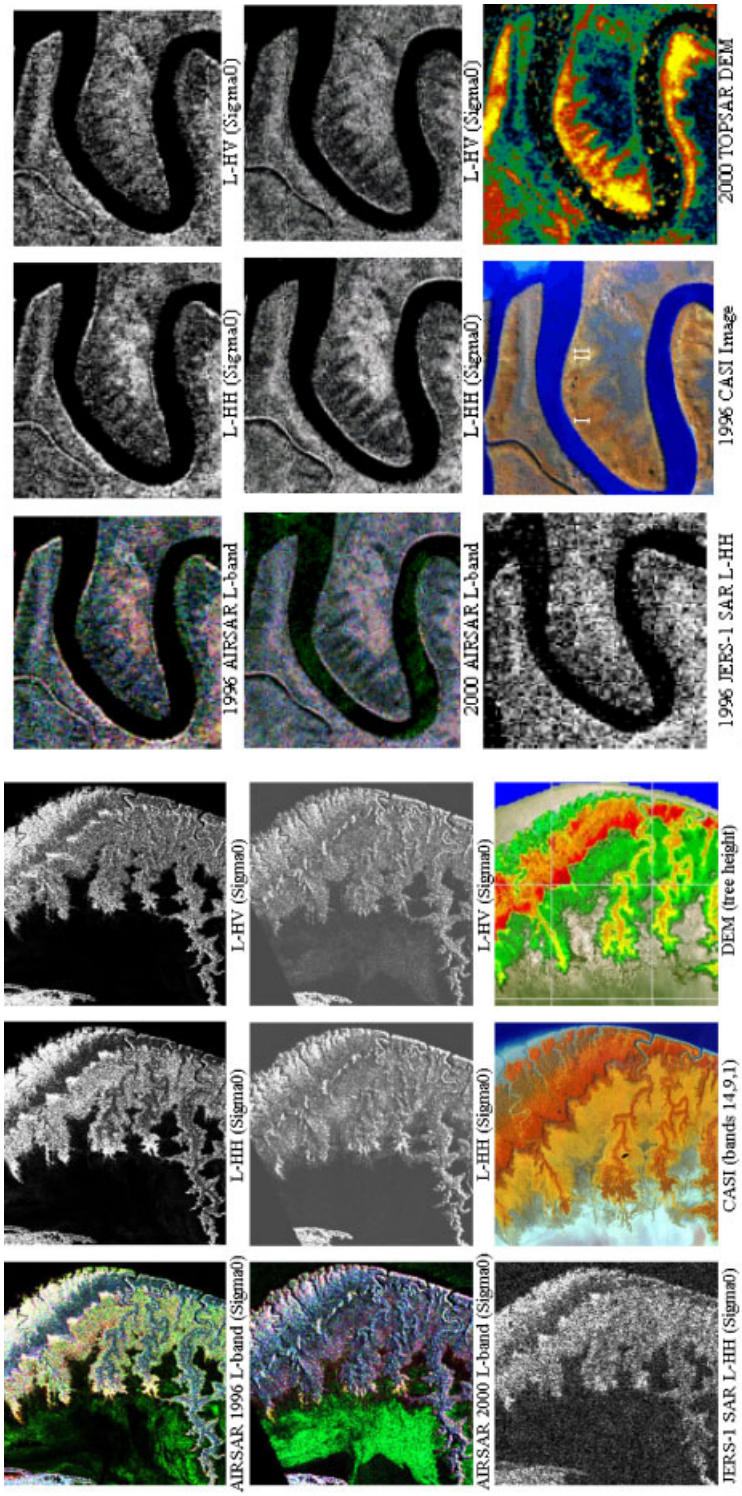

Figure 3. Subsets of AIRSAR L-band data (HH and HV shown separately) acquired in 1996 and 2000 and JERS-1 SAR HH images of mangroves along (a) the West Alligator River and (b) the Daintree River in northern Australia. Areas of mangrove dominated by different species are indicated in the CASI images. The DEM is derived using stereo aerial photography and TOPSAR C-band interferometry respectively. The higher (~20 m) mangroves are in orange/yellow and are dominated by *R. stylosa* at both sites.

DOI: 10.1002/aqc

when AIRSAR data were acquired, the zones observed could be associated with different species because of dominance by one or two in the upper canopy. However, detailed mapping of all species was difficult because many were rare, confined to isolated patches, or occurred in the subcanopy or understorey. Within the AIRSAR data acquired in 1996 (at an incidence angle of 36°), Zones I–IV were discernible, largely because the reduced L-band backscattering coefficient at HH and HV polarizations from the central spine of *R. stylosa* (Zone III) contrasted with the higher backscattering coefficient from the adjoining mangroves, particularly Zones II and IV. The extensive stands of *A. marina* (Zone I) also exhibited a higher backscattering coefficient compared with Zone III despite their relatively low stature. Zone V was not evident within the 1996 AIRSAR data because regeneration only occurred from the mid-1990s. All zones were less discernible within the 2000 AIRSAR L-band data, which were acquired at a higher incidence angle (approaching 70°). However, four zones could be differentiated using the 1994 JERS-1 SAR data acquired at an incidence angle of 33° and, as with the 1996 AIRSAR data, a lower backscattering coefficient was observed for Zone III.

The mangroves of the Daintree River exhibited a more complex zonation and stands dominated by a single species were less distinct within the CASI reflectance data. The height of these mangroves, when estimated using TOPSAR C-band interferometry (Held *et al.*, 2003), was generally less than 10 m although stands as high as 20 m and dominated by *R. stylosa* occurred. In contrast to the West Alligator mangroves, the larger *R. stylosa* forests dominated the seaward margins, particularly along the estuary, whilst a mix of *Ceriops* and *Bruguiera* occurred on the landward side, with height decreasing rapidly towards the saline flats and adjacent forest. In both 1996 and 2000 (Figure 3(b)), and as observed in the West Alligator mangroves, L-band backscattering coefficient at HH and HV polarizations was low within the high biomass *R. stylosa* stands, which was attributable to greater attenuation of microwaves by the canopy and prop roots. Greater double-bounce interactions probably caused the increase in the backscattering coefficient within the more open *Ceriops* complex. In 1996 and 2000, the look directions were towards the west and east respectively and these differences accounted for the slight enhancement of double-bounce scattering along opposite margins of the river banks. The tide was relatively low on both observation dates and so differences in inundation were not the cause. No significant changes in the L-band backscattering coefficient from the mangroves themselves were observed between dates which was attributable, in part, to the similarity in incidence angle (54° and 45° in 1996 and 2000 respectively). The contrast between communities was less within the JERS-1 SAR L-band HH data, partly because of speckle noise within the data and the coarser spatial resolution relative to the area and distribution of species within the mangroves. The zonation observed within the AIRSAR data over French Guiana was related more to the growth stage of forests, as species diversity was low. Some variation in L-band backscattering coefficient from mangroves at these sites was associated with tidal inundation, which enhanced the backscattering coefficient within the more open and/or lower mangroves on the coastal margin. Consistent mapping of mangrove zones was therefore complicated because of the variations associated with growth stage/form and also tidal inundation at the time of observation.

Structural attributes

Forest structure is assessed typically in relation to height, density and basal area (which relates to diameter distributions) in addition to the integrative value of above-ground biomass ($\mathrm{Mg\,ha^{-1}}$). The trends in L-band backscattering coefficient with mangrove forest height were therefore investigated by extracting data profiles from selected transects perpendicular to the seaward margin and comparing these with canopy height profiles from the same or similar locations. DEMs of mangrove canopy height were generated either from stereo photography (West Alligator River), SAR interferometry (Daintree River) or Light Detection and Ranging (lidar) data (French Guiana).

DOI: 10.1002/aqc

Within the West Alligator River mangroves, tree height increased towards the centre (maximum height of ~ 23 m) of the mangroves where *R. stylosa* dominated (Mitchell *et al.*, in press). Within this central zone, L-band HH and VV data were noticeably lower (~ -15 to -20 dB) in both the 1996 and 2000 data compared with adjacent zones (typically -8 to -13 dB). A similar reduction in L-band HH data was noted using JERS-1 SAR data acquired on three dates at an incidence angle of 33°. Even so, the L-band HH backscattering coefficient was greater from high *R. stylosa* forests along the uppermost reaches of creeks, which was attributed to the reduced extent and greater openness of the forests but also to differences in viewing angle. In all SAR data, the backscattering coefficient over the seaward zones was enhanced compared with those that were landward because of the more open canopy and increased double-bounce interactions. Similar interactions as well as the viewing angle were considered to be responsible for the larger values of backscattering coefficient along the height divide between the *R. stylosa* (Zone III; >20 m) and landward zones (Zones I–II; <6–10 m). Differences in L-band backscattering coefficient with incidence angle, particularly at cross-polarizations, were also noticeable. Within the Daintree River, the tallest mangroves (~ 25 m), which were also dominated by *R. stylosa*, were located close to the water's edge and similarly exhibited the lowest AIRSAR and JERS-1 SAR backscattering coefficient, particularly at co-polarizations. Towards the landward margins, the L-band HH backscattering coefficient increased with decreasing height, which was attributable to greater double-bounce interactions from the Ceriops-dominated forests. At Crique Fouillée and Sinnamary, tree height decreased towards the seaward margin from maximum values of ~ 27 m (Fromard *et al.*, 1998), but a relatively weak correspondence with the backscatttering coefficient was observed. For all sites, poor relationships were observed between backscattering coefficients and other structural measures, including basal area, tree diameter (cm) and density.

Biomass

The reduction in backscattering coefficient within the taller (and generally higher biomass) forests in northern Australia was unexpected given that most studies have observed an increase in backscatter with biomass until saturation occurs (i.e. where the slope of the biomass/backscatter coefficient curve approaches zero). At L-band, saturation levels for forests of between 30 and 140 Mg ha^{-1} have typically been reported (e.g. Luckman *et al.*, 1998; Fransson and Israelsson, 1999; Mougin *et al.*, 1999).

To evaluate the potential of L-band for biomass retrieval, above-ground biomass was estimated for the mangroves of the West Alligator River by applying the species-specific allometric equations of Clough and Scott (1989), Comley (2002) and Peter Brocklehurst (unpublished data) to available forest inventory data and related to SAR backscattering coefficient data. For French Guiana, the equations of Fromard *et al.* (1998) were used but insufficient field measurements were available for the Daintree and Perak mangroves.

For the West Alligator River, and using field data acquired in 2002, empirical relationships established between L-band backscatter and above-ground biomass (Mitchell, 2004) revealed an increase at all polarizations (Figure 4) until approximately 125 Mg ha^{-1}. However, a decline was observed thereafter such that the backscatter coefficient for forests greater than 250 Mg ha^{-1} and those of lower ($< \sim 50$–70 Mg ha^{-1}) biomass were similar. The extracted backscattering coefficient was also consistently higher at the lower (36°) incidence angle. Within Crique Fouillée, increases in backscatter with biomass to the saturation level were most evident at HV polarizations (see Figure 5) but declines at higher biomass levels were not observed and a more variable increase in co-polarized backscattering coefficient with biomass was evident. These observations suggest forest structure is an important determinant of the backscatter coefficient, particularly as the reduction in L-band HH within the higher biomass *Rhizophora*-dominated mangroves of northern Australia was not evident within mangroves of similar biomass in French Guiana. Where mapping is complicated by structural variation (Held *et al.*, 2003), the integration of other information (e.g. height, species classifications) can be used to identify such forests, in which

DOI: 10.1002/aqc

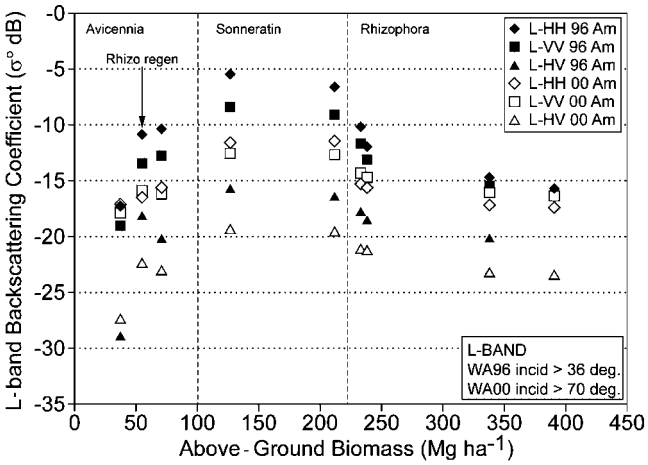

Figure 4. Relationships between L-band backscattering coefficient (σ°, dB) and the above-ground biomass of West Alligator River (WA) mangroves at different polarizations and incidence angles (based on 1996 and 2000 AIRSAR data).

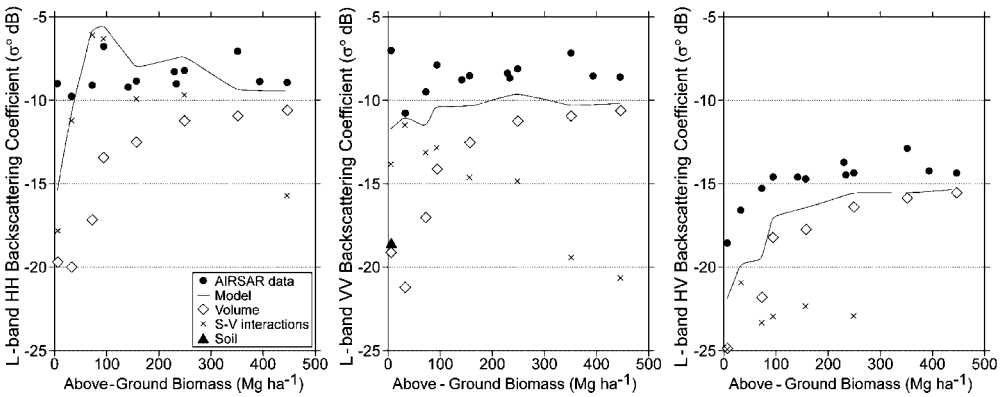

Figure 5. L-band SAR simulation of mangrove forest at Crique Fouillée, French Guiana. The main contribution to the HV polarization is from volume scattering. Soil–volume (S–V) interactions decline with increasing biomass.

case the decline in L-band backscattering coefficient after the saturation level could be used to differentiate biomass levels.

Several studies (e.g. Dobson *et al.*, 1992; Lucas *et al.*, 2004) have indicated that microwaves of differing frequency and polarization interact with, and can therefore be related to, the biomass of different forest components (e.g. leaves, roots). However, an understanding of microwave interaction with the forest volume has proved difficult to achieve using empirical relationships with SAR data because of inherent relationships between these components (Lucas *et al.*, 2000). The retrieval of component biomass is also more difficult in forests above the level of saturation (herein referred to as high biomass forests) as greater attenuation by the crown volume reduces the diversity of scattering mechanisms between components and also the ground surface compared with those below saturation (low biomass forests). Hence, less information on the forest biomass and structure (and therefore species, growth stage and form) can be extracted. However, by considering the scattering mechanisms operating within low and high forests separately, L-band SAR data can be better interpreted.

DOI: 10.1002/aqc

Within low biomass forests, microwaves can penetrate to the underlying surface, which typically consists either of the substrate (mud or sand) of varying moisture content or water of varying salinity. This greater interaction with the surface often leads to an enhancement of the backscattering coefficient by several decibels compared with the denser, closed canopy of many higher biomass forests (Proisy *et al.*, 2002). Similarly, a greater diversity of scattering mechanisms is often evident and the contribution of each can also be better related to specific biomass components (Lucas *et al.*, 2004). By parameterizing the SAR simulation model of Karam *et al.* (1995) with field data collected from Crique Fouillée (based on a mean incidence angle of 58°), Proisy *et al.* (2000) indicated that for stands supporting a biomass of $>30\,\mathrm{Mg\,ha^{-1}}$, L-band HH data were particularly sensitive to branch biomass, L-band VV data to trunk biomass and L-band HV data to leaf/branch biomass up to the level of saturation, which approximated $140\,\mathrm{Mg\,ha^{-1}}$. The different scattering mechanisms were suggested, with double-bounce branch and trunk (soil–vegetation) interactions dominating at L-band HH and VV in these low biomass forests, and volume scattering increasing for all polarizations up to the level of saturation (Figure 5; Proisy *et al.*, 2000). These simulations and observations suggest that ALOS PALSAR data (all polarizations) might be useful for retrieving the biomass of tree components within low biomass forests. As with the empirical models, the sensitivity of L-band HV data to total above-ground biomass was revealed and statistical inversion of these cross-polarized data up to the level of saturation could be achieved. The decrease in the soil-interaction term at L-band VV (above $\sim 20\,\mathrm{Mg\ ha^{-1}}$) and HV also appeared useful for biomass retrieval in these forests. As L-band HH and VV signals are attributable to soil–vegetation interactions and direct backscattering from the soil surface, statistical inversion for retrieving vegetation characteristics is strongly dependent upon a knowledge of soil properties, which is difficult to measure on the ground and hence is generally poorly simulated. Co-polarized L-band SAR data might therefore remain limited for biomass retrieval until the soil–vegetation interactions can be better determined (Proisy *et al.*, 2000). Similar outcomes were achieved when the same model was parameterized using data collected from the West Alligator River mangroves (Mitchell, 2004).

Within high biomass forests, microwaves at L-band interact with multiple branches of various sizes occurring within the upper forest canopy and volume scattering predominates, even at lower (e.g. P-band) frequencies (Mougin *et al.*, 1999), and saturation of the backscatter occurs. In addition, greater structural complexity in high biomass stands, including the formation of canopy gaps and the dieback/growth of canopy layers, and greater attenuation from a more established canopy may reduce the capacity for trunk–ground interactions and hence the magnitude of the backscatter coefficient, even where forests are inundated (Imhoff, 1995b). Mature forest composed of a high density of trunks and prop roots may interfere with the backscatter pathways and produce a low overall backscattering coefficient, as typified by the *R. stylosa* forests of northern Australia.

Change detection

The detection of change is important for monitoring the response of mangroves to prevailing coastal and climatic conditions and also for determining the extent of clearance and/or degradation as a result of human activity. Within the four study areas, mangroves were affected by natural and/or anthropogenic change. The mangroves of Kakadu NP and Daintree NP, as with many in these regions, are subject to both rapid (e.g. cyclone and storm damage) and gradual (e.g. sea-level variation) change (EPA, 1999; Duke *et al.*, 2001; Kirkwood and Dowling, 2002; Lucas *et al.*, 2002), although these are relatively small and often occur in linear configurations parallel to the coast or along creeks (Lucas *et al.*, 2002). Hence, they are only likely to be detected by comparing time-series of fine ($<5\,\mathrm{m}$) spatial resolution data. As with many mangroves along the 1600-km stretch of coast from the Amazon River to the Orinoco Delta, those in the French Guiana littoral are subject to both rapid and gradual change in response to predominantly natural factors, with successive erosion and sediment deposition phases controlling their establishment and mortality (Fromard *et al.*, 1998). Migration of giant mud banks is observed along much of the coast and is related in

DOI: 10.1002/aqc

part to variations in the substantial amount of sediment dispersed from the Amazon (Ronchail *et al*., 2002; Aalto *et al*., 2003; Allison and Lee, 2004; Baltzer *et al*., 2004). Significant changes have been observed using time-series of JERS-1 SAR, which have been supported by observations using historical aerial photography (Fromard *et al*., 2004) as well as SPOT HRVIR data. In Perak State, logging operations are commonplace whereby trees are cut from boats but stumps and branch debris are left behind. These logged areas exhibit a high L-band HH backscattering coefficient (and hence a bright appearance in the imagery) because of double-bounce interactions between the remaining tree trunks emerging above the substrate and/or water surface (Rosenqvist *et al*., 2007). Regeneration to a secondary growth state generally occurs within a few years, after which the distinction between mature and degraded forest becomes increasingly difficult in single-date SAR imagery, thus highlighting the need for repetitive monitoring of mangrove areas to ensure adequate tracing of changes. Multi-temporal SAR colour composites provide a simple but effective means for disturbance mapping, yielding a clear indication of both when changes occurred and the acreage affected.

POTENTIAL OF ALOS PALSAR FOR MANGROVE ASSESSMENT

Although focusing on tropical mangroves, the case studies outlined have provided an insight into the benefits of L-band SAR data for characterizing, mapping and monitoring mangroves across their geographical range. In this section, the potential use of the ALOS PALSAR data for mangrove assessment is discussed and a framework for mapping and monitoring through integration of these data is suggested.

Mapping mangrove extent, structure and biomass

A major benefit of the ALOS PALSAR is that coastal zones will be observed regardless of weather and illumination conditions and hence opportunities for characterizing, mapping and monitoring mangroves in areas with persistent cloud cover will be increased. The JAXA observation strategy also facilitates the generation of 50-m spatial resolution mosaic ALOS PALSAR images over large areas for wall-to-wall mapping of mangroves and contained zones. Finer (10–20 m) beam mode data sets are anticipated to provide opportunities for developing algorithms for mapping mangrove extent and zonation patterns as well as retrieving structural attributes and biomass. As data will be acquired systematically over similar time periods every year and at the same polarization and incidence angle, algorithms developed are more likely to be consistent and generally applicable within and between regions.

For algorithm development and validation, sites with ground data and finer spatial resolution images and image products (e.g. species maps, canopy height models), such as those described above, will play a key role in understanding the information content of these data. Existing approaches to characterization and mapping developed at such sites will need to be revisited, though, because of differences in sensor (e.g. JERS-1 SAR, AIRSAR) configuration and viewing angles as well as changes in the mangroves themselves (e.g. resulting from differences in tidal inundation or storm damage). Algorithm development should also consider data from other sensors (e.g. Landsat or SPOT) or sources (e.g. existing vegetation maps), as these can provide useful supplementary information (e.g. canopy cover and height).

A particular advantage of the ALOS PALSAR over its predecessor is that dual (HH and HV) rather than single polarization HH data alone are being acquired and for some areas quad polarized data will be available. The inclusion of L-band HV data, in particular, will provide increased opportunities for differentiating between different mangrove zones, whether composed of different species, growth stages or biomass levels (Lucas *et al*., 2006). Even so, the discrimination, mapping and attribution of mangrove zones will be complicated by differences in species and growth stage and *a priori* knowledge (e.g. from local surveys, classifications of optical data sets or reference to tidal records) of zonation sequences on a

DOI: 10.1002/aqc

site-by-site basis might be necessary for effective interpretation of these data. For example, existing classifications of mangrove communities will allow high biomass *R. stylosa* forest to be differentiated from low biomass forests and facilitate appropriate implementation of biomass retrieval algorithms. The provision of fully polarimetric data will also allow information on different scattering mechanisms to be extracted, thereby assisting retrieval of biophysical attributes (e.g. through parameter retrieval models), whilst the interferometric capability will present opportunities for tree height retrieval. For retrieval algorithms, mangrove height surfaces generated independently using a combination, for example, of stereo aerial photography, LiDAR and airborne interferometric SAR will be necessary, particularly for their calibration and validation, and this is planned under the K&C Initiative.

A recognized limitation of the 50-m PALSAR mosaics is that the spatial resolution may be too coarse to resolve detail, particularly where mangroves are fringing or fragmented although more expansive tracts will be observed. Similarly, the differentiation of mangrove zones and biomass classes will also be less achievable using regional mosaics. Image speckle (i.e. noise resulting from coherent scattering from random targets) is also likely to reduce the usefulness of the data, although this can be minimized using spatial and adaptive filters and averaging techniques (Zhang *et al*., 2002; Xiao *et al*., 2003). However, such processing will tend to degrade resolution and blur small objects (Oliver and Quegan, 2004) and might further limit the utility of the ALOS PALSAR data for mapping detail in mangroves and monitoring small changes in their extent and state.

Monitoring change

Data acquired by the ALOS PALSAR are anticipated to play an important role in monitoring in two ways. First, the annual or binannual time-series of data will allow the detection of change over the lifespan of the ALOS PALSAR and a sequence of at least one image per year over a 3-year period will be acquired globally. Second, comparisons of data and maps generated using ALOS PALSAR with those derived for the mid-1990s from the JERS-1 SAR (or other radar or optical remote sensing data sets) will facilitate the detection and mapping of decadal change. The 100-m spatial resolution JERS-1 SAR mosaics generated as part of the GRFM project will be ideally suited for this purpose. Change detection will be facilitated also by the geometric consistency of the data sets which overcomes many of the difficulties encountered previously when comparing data from different sensors and time-periods. Repeat observations at similar times of year will also reduce the variability in the backscatter associated with changing environmental conditions, although tidal influences will be more difficult to isolate.

The detection of change will depend upon the spatial extent and nature of change between the times of observation. Changes associated with extreme events (e.g. storm or tsunamis) or human disturbance (e.g. deforestation) are more likely to be identified compared with areas where these are more subtle (e.g. mangrove expansion and retraction associated with sea level rise). Change at the decadal level is anticipated to provide the most useful data set for mangrove monitoring as many areas would have experienced significant change, including that associated with natural processes, over such a time period. A particular advantage of comparing the L-band SAR data sets is that HH polarization data sets are available from both the JERS-1 SAR and ALOS PALSAR and these are internally consistent and compatible with each other, with the incidence angle being similar. The detection of change associated with deforestation is anticipated to be a major benefit of using time-series of ALOS PALSAR and JERS-1 SAR data. Notable though, is that most areas cleared after the last JERS-1 SAR acquisition and left subsequently for regeneration will most likely remain undetected in the ALOS PALSAR data unless ancillary data (including those acquired by optical sensors) acquired during the intervening time gap are available.

DOI: 10.1002/aqc

Mapping and monitoring strategies

To facilitate more efficient use of the regional and global mapping and monitoring strategy that the ALOS PALSAR is subject to, the following are recommended:

(a) The establishment of a global network of reference sites to support the interpretation of data acquired by the ALOS PALSAR. SAR data have already been acquired at a number of sites worldwide and can be used to understand and interpret the L-band data recorded by the ALOS PALSAR more effectively, particularly if used in conjunction with supportive field data as well as established wave scattering models. Finer spatial resolution data sets of mangrove extent, floristics, structure and biomass also represent important validation sets for products generated using ALOS PALSAR data.
(b) Investment in the development and validation of algorithms that facilitate routine, reliable and consistent mapping and monitoring of mangroves at regional to global scales. Few algorithms are currently available, largely because many studies on mangroves have focused on small areas and few comparisons have been made between sites.
(c) The identification and general provision of ancillary data sets (including JERS-1 SAR data) which are available to support national and international mapping and monitoring activities. In some countries, regional data sets of mangroves (e.g. distribution or zonation maps) already exist (e.g. Souza-Filho and Paradalla, 2003; Wrightman *et al.*, 2004) and these can provide a spatial framework around which a mapping and monitoring system can be developed. Additional data can also be integrated to support the mapping and monitoring of mangroves. For example, the 30–90 m spatial resolution global elevation data set acquired during the Shuttle Radar Topographic Mission (SRTM) can be used to approximate the mean canopy height (relative to sea level) of large, contiguous mangrove areas (Simard *et al.*, 2006) while optical remote sensing data can be used for refining regional maps of zonation and extent.
(d) The provision of avenues for coordinating mapping and monitoring activities, both nationally and internationally. The JAXA K&C Initiative is actively promoting the mapping and monitoring of mangroves at a regional level using the ALOS PALSAR data, but further scientific, logistical and financial support will be needed from a range of other organizations (e.g. governmental and non-governmental organizations, universities and industry) if these data are to be used effectively.

SUMMARY AND CONCLUSIONS

Based on the authors' own case studies and those published in the literature, the paper presents an overview of L-band SAR for mangrove assessment. From these findings, the usefulness of ALOS PALSAR data for mapping and monitoring mangroves has been evaluated in part, and strategies have been outlined for data analysis and integration during its stated operational lifetime of 3 years. Specifically, L-band SAR data alone have proved to be useful for mapping mangrove extent and zonation (as a function of structural differences between species and growth stages). Temporal datasets are useful also for detecting change, particularly when rapid and expansive. Potential for the retrieval of mangrove canopy height from interferometric SAR data and total and component (e.g. branch and trunk) biomass through empirical relationships and decomposition of polarimetric SAR data, respectively, has been suggested. However, inconsistencies in the interpretation of the data have also been identified, including those associated with the varying influences of tidal inundation and the underlying substrate, the forest structure itself (e.g. root systems), and the configuration of the sensor (e.g. incidence angle).

For characterizing mangroves across their geographical range, the JAXA K&C Initiative has promoted the production of global 50-m spatial resolution ALOS PALSAR mosaics on an annual or biannual basis

DOI: 10.1002/aqc

that can be used for mapping mangrove extent, zonations and biomass. Using these mosaics alone, short-term changes in mangroves will be detected whilst for mapping and monitoring change in the longer term, comparisons with historical JERS-1 SAR data are likely to be effective. In all cases, a coordinated approach to characterization, mapping and monitoring of mangroves using these data, as promoted under the K&C Initiative, is essential. The benefit of such an approach has been shown by our own case studies, whereby comparison between sites has demonstrated some consistencies in the L-band data (e.g. changes in backscattering coefficient with biomass, low backscattering coefficient from *R. stylosa* dominated forests) and suggested that algorithms for routine assessment from ALOS PALSAR data might be developed. In all cases, however, the integration of optical remote sensing and height data from other sensors will lead to better characterization and mapping of mangroves.

ACKNOWLEDGEMENTS

The authors would like to acknowledge the financial support and field assistance provided by the Environmental Research Institute of the Supervising Scientist (ERISS), particularly Kirrilly Pfitzner, and Parks Australia North (PAN) and technical support provided by the School of Surveying and Spatial Information Systems, the University of New South Wales. The JERS-1 data used in the study were provided by JAXA within the framework of the Global Rain Forest Mapping (GRFM) project. The authors also wish to acknowledge the support of local Aboriginal landowners in Kakadu NP. Acknowledgement is also extended to CSIRO Land and Water, NASA Jet Propulsion Laboratory and the Institut de Recherches pour le Développement in French Guiana. Finally, the two reviewers are thanked for the valuable contribution towards refining the manuscript.

REFERENCES

Aalto R, Maurice-Bourgoin L, Dunne T, Montgomery DR, Nittrouer C, Guyot JL. 2003. Episodic sediment accumulation on Amazonian floodplains influenced by El Niño/Southern Oscillation. *Nature* **425**: 493–497.

Allison MA, Lee MT. 2004. Sediment exchange between Amazon mudbanks and shore-fringing mangroves in French Guiana. *Marine Geology* **208**: 169–190.

Alongi DM. 2002. Present state and future of the world's mangrove forests. *Environmental Conservation* **29**: 331–349.

Askne JIH, Dammert PBG, Ulander MH, Smith G. 1997. C-band repeat-pass interferometric SAR observations of the forest. *IEEE Transactions on Geoscience and Remote Sensing* **35**: 25–35.

Baltzer F, Allison M, Fromard F. 2004. Material exchange between the continental shelf and mangrove-fringed coasts with special reference to the Amazon-Guianas coast. *Marine Geology* **208**: 115–126.

Blasco F, Janodet E, Bellan MF. 1994. Impacts of coastal hazards on mangroves in the Bay of Bengal. *Journal of Coastal Research* **12**: 277–288.

Blasco F, Saenger P, Janodet E. 1996. Mangroves as indicators of coastal change. *Catena* **27**: 167–178.

Brennan K. 1996. An annotated checklist of the vascular plants of the Alligator Rivers Region, NT, Australia. Supervising Scientist Report, No. 109. Supervising Scientist, Environment Australia, Canberra, Australia.

Castel T, Caraglio Y, Beaudoin A, Borne F. 2001. Using SIR-C SAR data and the AMAP model for forest attributes retrieval and 3-D stand simulation. *Remote Sensing of Environment* **75**: 279–290.

Cloude SR, Pottier E. 1997. An entropy based classification scheme for land applications of polarimetric SAR. *IEEE Transactions on Geoscience and Remote Sensing* **35**: 68–78.

Clough BF, Scott K. 1989. Allometric relationships for estimating above-ground biomass in six mangrove species. *Forest Ecology and Management* **27**: 117–127.

Comley BTW. 2002. Coastal mangrove wetland productivity and management, Darwin Harbour, Northern Territory, Australia. Masters thesis, NT University, Darwin.

Danielsen F, Sørensen MK, Olwig MF, Selvam V, Parish F, Burgess N, Hiraishi T, Karunagaran VM, Rasmussen MS, Hansen LB, Quarto A, Suryadiputra N. 2005. The Asian tsunami: a protective role for coastal vegetation. *Science* **310**: 643.

Dobson MC, Ulabym FT, LeToan T, Beaudoin A, Kasischke ES, Christensen N. 1992. Dependence of radar backscatter on coniferous forest biomass. *IEEE Transactions on Geoscience and Remote Sensing* **30**: 412–414.

DOI: 10.1002/aqc

Duke N, Roelfsema C, Tracey D, Godson L. 2001. Preliminary investigation into dieback of mangroves in the Mackay region: initial assessment and possible causes. Report to Queensland Fisheries Service, Northern Region (DPI) and the Community of Mackay Region.

EPA. 1999. State of the Environment, Queensland 1999. Environmental Protection Agency, Queensland Government, Brisbane.

Food and Agricultural Organization. 2003. Page: Global mangrove area estimate. www.fao.org/forestry/site/1720/en.

Fransson JES, Israelsson H. 1999. Estimation of stem volume in boreal forests using ERS-1 C- and JERS-1 L-band SAR data. *International Journal of Remote Sensing* **20**: 123–137.

Fromard F, Puig H, Mougin E, Marty G, Betoulle JL, Cadamuro L. 1998. Structure, above-ground biomass and dynamics of the French Guyana mangrove forest. *Oecologia* **115**: 39–53.

Fromard F, Vega C, Proisy C, 2004. Half a century of dynamic coastal change affecting mangrove shorelines of French Guiana. A case study based on remote sensing data analyses and field surveys. *Marine Geology* **208**: 265–280.

Fung AK, Li Z, Chen KS. 1992. Backscattering from a randomly rough dielectric surface. *IEEE Transactions on Geoscience and Remote Sensing* **30**: 356–369.

Gaveau DLW, Balzter H, Plummer S. 2003. Forest woody biomass classification with satellite-based radar coherence over 900 000 km^2 in Central Siberia. *Forest Ecology and Management* **174**: 65–75.

Held A, Ticehurst C, Lymburner L, Williams N. 2003. High resolution mapping of tropical mangrove ecosystems using hyperspectral and radar remote sensing. *International Journal of Remote Sensing* **24**: 2739–2759.

Hess LL, Melack JM, Simonett DS. 1990. Radar detection of flooding beneath the forest canopy: a review. *International Journal of Remote Sensing* **14**: 1313–1325.

Imhoff ML. 1995a. A theoretical analysis of the effect of forest structure on synthetic aperture radar backscatter and the remote sensing of biomass. *IEEE Transactions on Geoscience and Remote Sensing* **33**: 341–352.

Imhoff ML. 1995b. Radar backscatter and biomass saturation: ramifications for global biomass inventory. *IEEE Transactions on Geoscience and Remote Sensing* **33**: 511–518.

Karam MA, Amar F, Fung AK, Mougin E, Lopes A, Le Vine DM, Beaudoin A. 1995. A microwave polarimetric scattering model for forest canopies based on vector radiative transfer theories. *Remote Sensing of Environment* **53**: 16–30.

Kirkwood A, Dowling R. 2002. Investigation of mangrove dieback in the Pioneer River Estuary, Mackay. Report prepared by the Queensland Herbarium, Environmental Protection Agency, Queensland Government, Brisbane.

Krohn MD, Milton NM, Segal DB. 1983. Seasat synthetic aperture radar (SAR) response to lowland vegetation types in eastern Maryland and Virginia. *Journal of Geophysical Research* **88**: 1937–1952.

Li XW, Guo HD, Wang CL, Li Z, Liao JJ. 2003. DEM generation in the densely vegetated area of Hotan, north-west China using SIR-C repeat pass polarimetric SAR interferometry. *International Journal of Remote Sensing* **24**: 2997–3003.

Lucas RM, Milne AK, Cronin N, Witte C, Denham R. 2000. The potential of synthetic aperture radar (SAR) data for quantifying the above ground biomass of Australia's woodlands. *Rangeland Journal* **22**: 124–140.

Lucas RM, Ellison JC, Mitchell A, Donnelly B, Finlayson M, Milne AK. 2002. Use of stereo aerial photography for quantifying changes in the extent and height of mangroves in tropical Australia. *Wetlands Ecology and Management* **10**: 161–175.

Lucas RM, Moghaddam M, Cronin N. 2004. Microwave scattering from mixed-species forests, Queensland, Australia. *IEEE Transactions on Geoscience and Remote Sensing* **42**: 2142–2159.

Lucas RM, Cronin N, Lee A, Witte C, Moghaddam M. 2006. Empirical relationships between AIRSAR backscatter and forest biomass, Queensland, Australia. *Remote Sensing of Environment* **100**: 388–406.

Luckman A, Baker J, Honzak M, Lucas R. 1998. Tropical forest biomass density estimation using JERS-1 SAR: seasonal variation, confidence limits, and application to image mosaics. *Remote Sensing of Environment* **63**: 126–139.

MacDonald HC. 1980. Techniques and applications of imaging radar. In *Remote Sensing in Geology*, Siegel BS, Gillespie AR (eds). John Wiley: New York; Chapter 10.

Madsen SN, Zebker HA, Martin J. 1993. Topographic mapping using radar interferometry: processing techniques. *IEEE Transactions on Geoscience and Remote Sensing* **31**: 246–255.

Milne AK. 2000. PACRIM 2 Airsar deployment to the Asia-Pacific Region August–October 2000: Report on the data acquisition phase and early results. *Proceedings of the Asian Conference on Remote Sensing*, Taiwan, December 4–8, 2000. Asian Association of Remote Sensing (AARS), Centre for Space and Remote Sensing Research, Chinese Taipei Society of Photogrammetry and Remote Sensing, Taipei, Taiwan.

Milne AK, Tapley I. 2002. PACRIM science applications: a decade with AIRSAR. *Proceedings of the AIRSAR Earth Science and Applications Workshop*. NASA Jet Propulsion Laboratory, California Institute of Technology Pasodena California.

DOI: 10.1002/aqc

Mitchell A. 2004. Remote sensing techniques for assessment of mangrove forest structure, species composition and biomass and response to environmental change. PhD thesis, University of New South Wales, Sydney, Australia.

Mitchell AL, Lucas RM, Donnelly BE, Pfitzner K, Milne AK, Finlayson M. in press. A new map of mangroves for Kakadu National Park, Northern Australia, based on stereo aerial photography. *Aquatic Conservation: Marine and Freshwater Ecosystems*. DOI: 10.1002/aqc.818.

Mougin E, Proisy C, Marty G, Fromard F, Puig H, Betoulle JL, Rudant JP. 1999. Multifrequency and multipolarisation radar backscattering from mangrove forests. *IEEE Transactions on Geoscience and Remote Sensing* **37**: 94–102.

O'Grady AP, McGuinness KA, Eamus D. 1996. The abundance and growth of *Avicennia marina* and *Rhizophora stylosa* in the low shore zone of Darwin Harbour, Northern Territory. *Australian Journal of Ecology* **21**: 272–279.

Oliver C, Quegan S. 2004. *Understanding Synthetic Aperture Radar Images*. SciTech Publishing Inc.: Raleigh, NC.

Ormsby JP, Blanchard BJ, Blanchard AJ. 1985. Detection of lowland flooding using active microwave systems. *Photogrammetric Engineering and Remote Sensing* **51**: 317–328.

Pasqualini V, Iltis J, Dessay N, Lointier M, Guelorget O, Polidori L. 1999. Mangrove mapping in North-Western Madagascar using SPOT-XS and SIR-C radar data. *Hydrobiologia* **413**: 127–133.

Pope KO, Rejmankova E, Paris JF, Woodruff R. 1997. Detecting seasonal flooding cycles in marshes of the Yucatan peninsula with SIR-C polarimetric radar imagery. *Remote Sensing of Environment* **59**: 157–166.

Proisy C, Mougin E, Fromard F, Rudant JP. 1998. Radar imaging of the mangroves in French Guiana. *Photo-Interprétation—Images Aériennes et spatiales* (Special Issue: Remote sensing and vegetation seminar) **36**: 81–88.

Proisy C, Mougin E, Fromard F, Karam MA. 2000. Interpretation of polarimetric radar signatures of mangrove forests. *Remote Sensing of Environment* **71**: 56–66.

Proisy C, Mougin E, Fromand F, Trichon V, Karam MA. 2002. On the influence of canopy structure on the polarimetric radar response from mangrove forest. *International Journal of Remote Sensing* **23**: 4197–4210.

Pulliainen J, Engdahl M, Hallikainen M. 2003. Feasibility of multi-temporal interferometric SAR data for stand-level estimation of boreal forest stem volume. *Remote Sensing of Environment* **85**: 397–409.

Ranson KJ, Sun G, Weishampel JF, Knox RG. 1997. Forest biomass from combined ecosystem and radar backscatter modeling. *Remote Sensing of Environment* **59**: 118–133.

Ronchail J, Cochonneau G, Molinier M, Guyot JL, De Miranda Chaves AG, Guimarães V. de Oliveira E. 2002. Interannual rainfall variability in the Amazon basin and sea-surface temperatures in the equatorial Pacific and the tropical Atlantic Oceans. *International Journal of Climatology* **22**: 1663–1686.

Rosenqvist A, Shimada M, Chapman B, Freeman A, De Grandi G, Saatchi S, Rauste Y. 2000. The Global Rain Forest Mapping project—a review. *International Journal of Remote Sensing* **21**: 1375–1387.

Rosenqvist A, Shimada M, Igarashi T, Watanabe M, Tadono T, Yamamoto H. 2003. Support to multi-national environmental conventions and terrestrial carbon cycle science by ALOS and ADEOS-II—the Kyoto & Carbon Initiative. *Proceedings of the International Geoscience and Remote Sensing Symposium* (*IGARSS '03*), Toulouse, France, July 21–25, 2003. Institute of Electrical and Electronics Engineers (IEEE), Geoscience and Remote Sensing Society (GRSS), USA.

Rosenqvist A, Shimada M, Watanabe M, Tadono T, Yamauchi K. 2004a. Implementation of systematic data observation strategies for ALOS PALSAR, PRISM and AVNIR-2. *Proceedings of the International Geoscience and Remote Sensing Symposium* (*IGARSS '04*), Anchorage, USA, September 20–24, 2004. Institute of Electrical and Electronics Engineers (IEEE), Geoscience and Remote Sensing Society (GRSS), USA.

Rosenqvist A, Shimada M, Chapman B, McDonald K, De Grandi G, Jonsson H, Williams C, Rauste Y, Nilsson M, Sango D, Matsumoto M. 2004b. An overview of the JERS-1 SAR Global Boreal Forest Mapping (GBFM) project. *Proceedings of the International Geoscience and Remote Sensing Symposium* (*IGARSS '04*), Anchorage, USA, September 20–24, 2004. Institute of Electrical and Electronics Engineers (IEEE), Geoscience and Remote Sensing Society (GRSS), USA.

Rosenqvist A, Finlayson M, Lowry J, Taylor D. 2007. The potential of long-wavelength satellite-borne radar to support implementation of the Ramsar Wetlands Convention. *Aquatic Conservation*: *Marine and Freshwater Ecosystems* **17**: 229–245.

Saatchi S, Agosti D, Alger K, Delabie J, Musinsky J. 2001. Examining fragmentation and loss of primary forest in the Southern Bahian Altantic forest of Brazil with radar imagery. *Conservation Biology* **15**: 867–875.

Schmullius CC, Evans DL. 1997. Synthetic aperture radar (SAR) frequency and polarization requirements for applications in ecology, geology, hydrology, and oceanography: a tabular status quo after SIR-C/X-SAR. *International Journal of Remote Sensing* **18**: 2713–2722.

Simard M, De Grandi G, Saatchi S, Mayaux P. 2002. Mapping tropical coastal vegetation using JERS-1 and ERS-1 radar data with a decision tree classifier. *International Journal of Remote Sensing* **23**: 1461–1474.

Simard M, Zhang K, Rivera-Monroy VH, Ross MS, Ruiz PL, Castaneda-Moya E, Twilley RR, Rodriguez E. 2006. Mapping height and biomass of mangrove forests in the Everglades National Park with SRTM elevation data. *Photogrammetric Engineering and Remote Sensing* **72**: 299–311.

Souza-Filho PWM, Paradella WR. 2003. Use of synthetic aperture radar for recognition of coastal geomorphological features, land-use assessment and shoreline changes in Braganca coast, Para, Northern Brazil. *Annals of the Brazilian Academy of Sciences* **75**: 341–356.

Spalding M, Blasco F, Field C. 1997. *World Mangrove Atlas*. International Society for Mangrove Ecosystems: Okinawa, Japan.

Storrs MJ, Finlayson M. 1997. Overview of the conservation status of wetlands of the Northern Territory. Supervising Scientist Report No. 116, Supervising Scientist, Environment Australia, Canberra, Australia.

Sun G, Ranson KJ. 1995. A three-dimensional radar backscatter model of forest canopies. *IEEE Transactions on Geoscience and Remote Sensing* **33**: 372–382.

Treuhaft RN, Cloude SR. 1999. The structure of oriented vegetation from polarimetric interferometry. *IEEE Transactions on Geoscience and Remote Sensing* **37**: 2620–2624.

Tsolmon R, Tateishi R, Tetuko JSS. 2002. A method to estimate forest biomass and its application to monitor Mongolian Taiga using JERS-1 SAR. *International Journal of Remote Sensing* **23**: 4971–4978.

Wrightman G, Danaher K, Dunning M, Beumer J, Michie M. 2004. Mangroves. In *National Oceans Office*. *Description of Key Species Groups in the Northern Planning Area*. National Oceans Office: Hobart.

Xiao J, Li J, Moody A. 2003. A detail-preserving and flexible adaptive filter for speckle suppression in SAR imagery. *International Journal of Remote Sensing* **24**: 2451–2465.

Zhang Z, Prinet V, Ma S. 2002. A new method for SAR speckle reduction. *Proceedings of the International Geoscience and Remote Sensing Symposium (IGARSS '02)*, Toronto, Canada, June 24–28, 2002. Institute of Electrical and Electronics Engineers (IEEE), Geoscience and Remote Sensing Society (GRSS), USA.

DOI: 10.1002/aqc